Journal of Sound and Vibration (1997) **199**(3), 349–368

DEVELOPMENT AND MODIFICATION OF A UNIFIED BALANCING METHOD FOR UNSYMMETRICAL ROTOR–BEARING SYSTEMS

Y. KANG, G.-J. SHEEN AND S.-M. WANG

Department of Mechanical Engineering, *Chung Yuan Christian University*, *Chung Li* 32032, *Taiwan*, *Republic of China*

(*Received* 17 *February* 1996, *and in final form* 3 *June* 1996)

On the basis of theoretical developments, this study proposes procedures for a modified unified balancing method for unsymmetrical rotor–bearing systems. A formulation of modal influence coefficient matrices is derived from the motion equations for unsymmetrical rotors, using a complex co-ordinate representation and the finite element method. Due to unequal properties in two principal directions, two sets of modal influence coefficients are presented. This formulation indicates that two trial masses in different directions are required in the two trial operations for each balancing plane. Also, the modal influence coefficients are found to be correlated with forward precession and unbalanced forces when asymmetry of bearings is considered. Therefore, forward precessions instead of measured displacements are required to calculate the unbalance distribution. Several examples are presented to verify the validity of the present work.

1. INTRODUCTION

Several successful methods for balancing flexible rotor–bearing systems have been developed. These methods can be differentiated into two groups which are concisely classified as the influence coefficient and modal methods.

The influence coefficient balancing method uses known trial masses to experimentally determine the sensitivity of a rotor–bearing system and subsequently calculates a set of discrete correction masses that will minimize whirl responses. In conventional procedures a trial mass is first applied to one of the balancing planes and the rotor responses are measured. This process is repeated for all of the other balancing planes, and then influence coefficient matrix is obtained from this data.

The early research in rotor balance was conducted by Thearle [1] and then Baker [2]. Their method was essentially a two-plane, two-sensor, single-speed, exact-point influence coefficient balancing procedure. Goodman [3] extended the influence coefficient procedure to include the least-squares method for balancing flexible rotor–bearing systems. Although the method had been known and published, it was more an art than a science. It is important, however, to evaluate the method because it is widely used and gives satisfactory results. Lund and Tonneson [4] examined the validity and accuracy of the influence coefficient method and investigated the influence of various instruments on the accuracy of the experiments. Tessarzik *et al*. experimentally evaluated the balancing precision of the influence coefficient method by the exact-point speed procedure [5] and the least squares procedure [6]. Linear programming techniques were employed by Pilkey and Bailey [7] for regulating the balance weight magnitudes and by Pilkey *et al*. [8] for locating optimal

0022–460X/97/030349 + 20 $25.00/0/sv960652

balancing planes through constraint equations. The influence coefficient method has become a practical balancing approach due to the advent of newer types of sensors, signal processing equipment and computers.

The modal balancing method uses graduated procedures in which the unbalance in each mode is corrected in turn, beginning with the first mode. At each stage the residual modal unbalance—that is, the initial unbalance in the mode plus the modal effect of any corrections made to the lower modes— is determined by a modal interpretation of the shaft vibration for a speed approximating the corresponding critical speed. In brief, the modal procedure consists of balancing successive modes of the rotor–bearing systems, individually, with a set of masses specifically selected so as not to disturb the previously corrected lower modes. By contrast, the influence coefficient procedure consists of determining correction masses in a predetermined set of planes, which will minimize measured vibrations at a series of sensors and speeds as predicted by influence coefficients relating vibration readings to mass additions; whereas the modal balancing method places more emphasis on physical insight into and understanding of the modal characteristics of the rotor–bearing systems.

The modal balancing methods are based on the mathematical models and modal analysis; and unbalance responses, intrinsic unbalance distribution and correction masses are expressed by the modal expansion at each critical speed of operation. Bishop and Gladwell [9] and Bishop and Parkinson [10] utilized planar modes which do not include the gyroscopic effect of a rotating disk, as well as cross-coupling and the asymmetric characteristics of support bearings. Thus, these assumed modes do not satisfy the rotor–bearing systems which have large disks, strongly asymmetric supports and/or other asymmetric effects. However, these assumed planar modes are still quite accurate, particularly for lightly damped systems supported by rolling bearings (Parkinson *et al*. [11, 12]).

The modal balancing method modified by Saito and Azuma [13] involves the theoretical introduction of a complex modal method. Meacham *et al*. [14] extended the complex modal method to include the contributions of residual bow effects. This procedure requires an accurate mathematical model of the rotor–bearing system in order to be balanced. As a result, this method may not be suited to many balancing situations.

Parkinson *et al*. [15] presented the similarities between the two balancing methods by examining both techniques in detail, thus providing the first exposition of the unified approach. Subsequently, Darlow *et al*. [16] proposed and implemented a demonstration of a unified balancing method. This method is designed to incorporate the best features of the influence coefficient and modal methods and also to reduce the disadvantages. The procedure essentially utilizes modal trial mass sets and modal correction mass sets, which are calculated on the basis of the modal influence coefficient obtained by taking data from trial operations. These mass sets will not contribute unbalance to the lower modes which have already been balanced. The process is continued by balancing successive modes by observations made with the rotor rotating at speeds which approximate the associated critical speeds. This method depends less on the physical insight provided by the modal interpretation of the rotor–bearing system. Essentially, the unified method is not restricted to planar modes and it is suitable for an automatic balancing process.

Darlow [17] described and discussed the three balancing methods in detail, including the analytical basis and specific implementation procedures. He indicated the relative superiority of the unified balancing approach.

Other important reports on analytical and experimental investigations involving influence coefficient, modal and unified balancing methods were surveyed by Darlow [18].

In general, the components of a rotor–bearing system, such as shafts, disks and bearings, are not axisymmetrical. Because of the non-axisymmetry, shafts and disks will have different stiffnesses and moments of inertia, in two principal directions. For example, a two-pole generator, a fluted cutter or drill bits, a lead screw, a flat shaft, a shaft with a key-way or coupling, a shaft with transversal cracks, and a large turbogenerator with marked mis-attachment all have variable stiffnesses in different directions due to their non-axisymmetrical area cross-section. A two-blade propeller, a fan or pump impeller, a teetered wind turbine, a cam shaft, and a rotary plow all have unequal rotary inertia about two principal axes of the non-axisymmetrical disk. However, studies of balance in unsymmetrical rotor–bearing systems have been very rare.

In the conventional unified methods, a single trial mass applied to each balancing plane with measured displacements is employed to calculate modal influence coefficients and modal unbalance distribution. Since the conventional method disregards the unequal properties of rotating parts and asymmetry of bearings, it cannot provide an equivalent unbalance distribution. In a previous study, a formulation of influence coefficients of unsymmetrical rotor–bearing systems was derived by Kang *et al*. [19], using a complex co-ordinate representation. On the basis of this new formulation, a modified influence coefficient method was also developed. In this method, two trial masses are applied on every balancing plane. Then, the forward precession calculated from the measurement of unbalanced responses is used to determine influence coefficients and unbalance distribution. The theoretical introduction for the influence coefficient method is also valid for the unified method. Thus this study formulates a modified unified approach from the finite element equations of unsymmetrical rotor–bearing systems. This approach is developed and verified as follows.

2. MODAL INFLUENCE COEFFICIENT MATRICES VIA FINITE ELEMENT EQUATIONS

The finite element method is well-developed and widely used in rotordynamics. Two different formulations of the complex-form equations were presented by Nelson [20] and Genta [21]. They defined the sign convention for angular co-ordinates with different choices. The latter one has the advantage of leading to real matrices in the case of a symmetrical system. Genta also presented finite element formulations for modelling unsymmetrical rotor–bearing systems. The motion equation considered the presence of deviatoric characteristics of non-axisymmetrical parts.

The displacement vector $\{p\} = (v, \theta_w, w, \theta_v)^{\mathrm{T}}$ of a typical rotor station for a finite element model is shown in Figure 1. It consists of two translations (v, w) and two rotations (θ_v, θ_w) in the transverse directions V and W of the rotating frame of reference. The directions V and W are defined relative to the inertial frame of reference by a constant rotating speed Ω about the U-axis and are attached to the cross-section of the shaft.

For rotating frame co-ordinates the motion equation of a non-axisymmetrical rotor and axisymmetrical bearings system can be expressed in the form:

$$[M]\{\ddot{p}\} + ([C]+\Omega[G])\{\dot{p}\}+[K]\{p\} = \{F_r\}+(\{F_c\}\cos\Omega t+\{F_s\}\sin\Omega t), \tag{1}$$

where $[M]$, $[C]$, $[G]$ and $[K]$ are system coefficient matrices. The two force terms in equation (1) are the rotating force $\{F_r\}$ due to an unbalance distribution and the non-rotating forces $\{F_c\}$ and $\{F_s\}$ due to stationary forces. The rotating force $\{F_r\}$ is a constant vector and is proportional to Ω^2. The formulation and assembling of this equation were presented by Kang *et al*. [19].

The solution to the unbalance response is then determined by

$$[K^s]\{p\} = \{F_r\}. \tag{2}$$

In this case only stiffness matrices are considered for determining unbalance distribution and whirl responses.

In the rotating reference frame, the complex co-ordinates and their complex conjugates are defined by

$$\{r\} = \{g\} + \mathrm{i}\{\gamma\}, \tag{3a}$$

and

$$\{s\} = \{g\} - \mathrm{i}\{\gamma\}, \tag{3b}$$

where $\{g\}$ and $\{\gamma\}$ denote the column vectors $(v, \theta_w)^{\mathrm{T}}$ and $(w, -\theta_v)^{\mathrm{T}}$, respectively. Then, equation (2) can be expressed in a complex form as

$$[R]\{r\}+[S]\{s\} = \{P\}, \tag{4}$$

where $\{R\} = \{R_1\}+\{R_2\}\mathrm{i}$ is assembled by the mean matrices, $\{S\} = \{S_1\}+\{S_2\}\mathrm{i}$ is assembled by the deviatoric matrices, and $\{P\} = \{P_v\}+\{P_w\}\mathrm{i}$ is the complex form of the unbalance force $\{F_r\}$.

Rearranging and expanding equation (4) gives

$$([A^{\mathrm{R}}]+[A^{\mathrm{I}}]\mathrm{i})(\{P_v\}+\{P_w\}\mathrm{i})+([B^{\mathrm{R}}]+[B^{\mathrm{I}}]\mathrm{i})(\{P_v\}-\{P_w\}\mathrm{i}) = [A]\{P\}+[B]\{Q\} = \{r\}, \tag{5}$$

where $\{Q\}$ is the complex conjugate of $\{P\}$, and details of $[A]$ and $[B]$ are shown in the report by Kang *et al*. [19]. The mathematical process from equation (4) to equation (5) gives two influence coefficient matrices for the unsymmetrical systems with axisymmetrical bearings. Correspondingly, influence coefficient matrices are obtained from the finite element equation which is expressed in the rotating frame of reference.

Not all degrees of freedom (DOF) of a finite element model can be measured, and only a few of the unbalanced forces belong to balancing planes. Both the number of balancing planes and measuring sensors are always smaller than the number of nodes. Retaining the DOF of the measured responses and balancing forces, and expanding equation (5), one obtains.

$$\sum_{j=1}^{J} (A_{kj}P_j + B_{kj}Q_j) = r_k, \quad k = 1, \ldots, K, \tag{6}$$

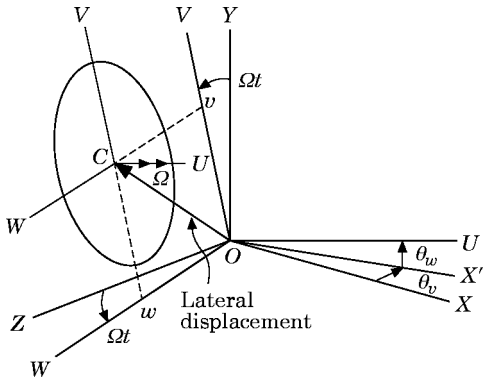

Figure 1. The displacement of a typical rotor station.

where J is the number of balancing planes and K is the number of measured points. When a trial mass is applied on the jth balancing plane, the kth measured response r_k is related to the balancing forces P_j and Q_j by the influence coefficients A_{kj} and B_{kj} respectively.

The unified approach uses the critical speed as a balancing speed to balance the rth mode. At this critical speed the unbalance whirl is inherently a modal shape. Only a few measurement points which are not located at the nodal point (including all points have a resonant response near zero) are needed to determine the relationship between resonant whirl and unbalance, since the resonant whirl has a fixed feature of the modal shape associated with this critical speed.

At the critical speed of the nth mode, equation (5) may be expressed by

$$[A_n]\{P\}+[B_n]\{Q\} = \{r_n\}, \tag{7}$$

where $[A_n]$ and $[B_n]$ are modal influence coefficient matrices. The elements of these matrices are determined by a sensitivity analysis between the resonant response and the trial masses.

When the systems have non-axisymmetrical bearings, the assembled equations of the rotor–bearing system have the form

$$[M^s]\{\ddot{p}\}+([C^s]+[C_c]\cos 2\Omega t+[C_s]\sin 2\Omega t)\{\dot{p}\}$$
$$+([K^s]+[K_c]\cos 2\Omega t+[K_s]\sin 2\Omega t)\{p\} = \{F_r\}+\{F_c\}\cos \Omega t+\{F_s\}\sin \Omega t \tag{8}$$

in the rotating frame. This time-varying equation has periodic coefficients with a frequency of 2Ω. The deviatoric stiffness and deviatoric damping of non-axisymmetrical bearings induce, in turn, $[K_c]$, $[K_s]$, $[C_c]$, and $[C_s]$.

For non-axisymmetrical bearings the synchronous whirl follows an elliptical orbit which includes forward precession and backward precession. The synchronous whirl can be expressed as

$$y_{sy}(t) = y_c \cos \Omega t + y_s \sin \Omega t,$$
$$z_{sy}(t) = z_c \cos \Omega t + z_s \sin \Omega t. \tag{9}$$

A complex form can then be defined as

$$q = y_{sy} + \mathrm{i}z_{sy} = f\mathrm{e}^{\mathrm{i}\Omega t} + b\mathrm{e}^{-\mathrm{i}\Omega t}, \tag{10}$$

where f and b are the forward and backward components of the synchronous whirl respectively.

Kang *et al*. [19] have verified that the influence coefficient matrices of unsymmetrical rotors with non-axisymmetrical bearings are correlated by the forward precession of the synchronous whirl and the unbalance force. At the critical speed of the nth mode, the relationship between forward components and unbalance is

$$[A_n]\{P\}+[B_n]\{Q\} = \{f_n\}, \tag{11}$$

where $\{f_n\}$ is a vector of forward components at measurement points.

3. THE DETERMINATION OF MODAL TRIAL MASS SETS

The unified approach uses a modal balancing method for adding correction masses in modal sets. Compared to the modal method, the unified method has the advantage that prior knowledge of the dynamic characteristics of the rotor–bearing system is not required.

Essentially, the unified method derives the modal correction mass sets by the determination of modal influence coefficients. This technique involves the calculation of modal trial mass sets, as outlined by Parkinson *et al*. [15]. Both modal trial mass sets and modal correction mass sets are determined in such a way as to affect the mode of interest while not affecting the lower modes which have already been balanced.

The n correction masses of $m_1c_1, m_2c_2, \ldots, m_nc_n$ are needed for balancing the nth mode, which can be expressed by

$$m_jc_j = \lambda_j m_1 c_1 \quad (j = 2, 3, \ldots, n), \tag{12}$$

where $\lambda_2, \lambda_3, \ldots$, are complex multipliers. These multipliers fix the relative magnitudes of modal correction masses. The associated trial masses must be scaled in accordance with the trial mass set, thus having a form of

$$\{P\}_n = (P_1, P_2, \ldots P_n)^{\mathrm{T}} = (1, \lambda_2, \ldots \lambda_n)^{\mathrm{T}} P_{1n} = \{\lambda\}_n P_{1n} \tag{13a}$$

for the nth mode. The complex conjugate of this trial mass set can be expressed by

$$\{Q\}_n = (Q_1, Q_2, \ldots Q_n)^{\mathrm{T}} = (1, \overline{\lambda}_2, \ldots \overline{\lambda}_n)^{\mathrm{T}} Q_{1n} = \{\overline{\lambda}\}_n Q_{1n}, \tag{13b}$$

where $\overline{\lambda}$ is the complex conjugate of λ. The symbols $\{\lambda\}_n$ and $\{\overline{\lambda}\}_n$ designate trial mass multiplier sets for the nth mode.

At the stage required for balancing the rth mode, the first $(n-1)$ modes will have been balanced, so that the relative magnitudes of correction masses in sets are satisfied, so that no fresh unbalance is produced in the lower $(n-1)$ modes. Thus the nth modal trial mass set does not deduce the first $n-1$ resonant whirl. For only one measurement point, it satisfies

$$\begin{aligned}
\underset{1\times n}{\lfloor A_1 \rfloor}\underset{n\times 1}{\{P\}}_n + \underset{l\times n}{\lfloor B_1 \rfloor}\underset{n\times 1}{\{Q\}}_n &= 0,\\
\underset{1\times n}{\lfloor A_2 \rfloor}\underset{n\times 1}{\{P\}}_n + \underset{l\times n}{\lfloor B_2 \rfloor}\underset{n\times 1}{\{Q\}}_n &= 0,\\
&\vdots\\
\underset{1\times n}{\lfloor A_{n-1} \rfloor}\underset{n\times 1}{\{P\}}_n + \underset{l\times n}{\lfloor B_{n-1} \rfloor}\underset{n\times 1}{\{Q\}}_n &= 0.
\end{aligned} \tag{14}$$

These above $(n-1)$ equations can be assembled into

$$\underset{(n-1)\times n}{[A]}\underset{n\times 1}{\{P\}}_n + \underset{(n-1)\times n}{[B]}\underset{n\times 1}{\{Q\}}_n = \underset{(n-1)\times 1}{\{0\}} \tag{15a}$$

or

$$[A]\{\lambda\}_n P_{1n} + [B]\{\overline{\lambda}\}_n Q_{1n} = \{0\}. \tag{15b}$$

The n trial masses can be scaled in accordance with equation (15b) by the multiplier set $\{\lambda\}_n$, which remains the determination of their absolute magnitudes.

When mode shapes are planar, the total deflection shape may approximately resemble a mode shape, if the rotating speed approximates the corresponding critical speed. For this reason there is no need to calculate the principal modes before balancing, and there is no need to measure the deflections along the shaft length. From observation of the resonant whirl, one needs merely to measure the unbalance response of one typical point with a large deflection. This unbalance response is used to determine a trial mass set which has no influence on lower modes.

If the damping is more complex and heavy, then the damped modes are likely to be non-planar; and the deflection shape of the unbalance whirl may not be a plane curve and it not a mode shape. A large number of measurement points along the shaft length are

needed to observe the deflection shape of this shaft. The total deflection shape due to unbalance is not a mode shape, even if the speed is equal to the corresponding critical speed. One may, however, use a trial mass set to insure that this set does not deduce the first $n-1$ resonant whirls. For N measurement point, it satisfies

$$\begin{gathered}
[\underset{N\times n}{A_1}]\{\underset{n\times 1}{P}\}_n + [\underset{N\times n}{B_1}]\{\underset{n\times 1}{Q}\}_n = \{\underset{N\times 1}{0}\},\\
[\underset{N\times n}{A_2}]\{\underset{n\times 1}{P}\}_n + [\underset{N\times n}{B_2}]\{\underset{n\times 1}{Q}\}_n = \{\underset{N\times 1}{0}\},\\
\vdots\\
[\underset{N\times n}{A_{n-1}}]\{\underset{n\times 1}{P}\}_n + [\underset{N\times n}{B_{n-1}}]\{\underset{n\times 1}{Q}\}_n = \{\underset{N\times 1}{O}\}.
\end{gathered} \tag{16}$$

Equation (16) can be assembled into the following form:

$$\lfloor\_A\_\rfloor\{P\}_n + \lfloor\_B\_\rfloor\{Q\}_n = \lfloor\_A\_\rfloor\{\lambda\}_n P_{1n} + \lfloor\_B\_\rfloor\{\bar{\lambda}\}_n Q_{1n} = \{0\}, \tag{17}$$

where

$$\lfloor\_A\_\rfloor = \begin{bmatrix} [A_1] \\ [A_2] \\ \vdots \\ [A_{n-1}] \end{bmatrix}, \qquad \lfloor\_B\_\rfloor = \begin{bmatrix} [B_1] \\ [B_2] \\ \vdots \\ [B_{n-1}] \end{bmatrix}$$

and their dimension is $N(n-1)$ rows and n columns. Only when $n=2$ and $N=2$ are $\lfloor\_A\_\rfloor$ and $\lfloor\_B\_\rfloor$ square matrices. In other cases the trial mass multiplier set cannot be exactly determined from equation (17). One may define an error function as

$$\{e\} = \lfloor\_A\_\rfloor\{\lambda\}_n P_{1n} + \lfloor\_B\_\rfloor\{\bar{\lambda}\}_n Q_{1n}, \tag{18}$$

where $\{\lambda\}_n$ and $\{\bar{\lambda}\}_n$ can be obtained by determining the minimization of $\{e\}^T\{e\}$. If all the $n-1$ mode shapes are planar, this minimum value is zero.

In this calculation, the scales of the trial masses can be obtained. The desired correction mass sets have the same scales as these trial mass sets, and their absolute magnitudes can then be determined by the trial operations.

4. BALANCING PROCESS OF THE MODIFIED UNIFIED METHOD

The unified balancing method is a progressive, graduated approach. The rotor is first operated at a speed of Ω_1, approaching the first critical speed ω_1, which is such that the whirl is clear, showing a resonance in the first mode. The addition of a correction mass to balance the first mode of unbalance thus not only results in a first mode unbalance which is zero, but it also affects many of the unbalance components in the higher modes. Once the first mode has been balanced it will normally be possible to run the rotor up to a speed Ω_2 approximating the second critical speed ω_2, at which stage a resonant whirl in the second mode is likely. This can be corrected by using two correction masses located at two planes along the rotor. These masses cancel the resultant unbalance component in the second mode, which contains the initial unbalance component together with the effect of the first mode correction, while these correction masses will not contribute unbalance to the first mode. This process is continued by balancing successive moves with the shaft rotating at speeds Ω_3, Ω_4, , . . approximating the associated critical speed ω_3, ω_4, . . . using, at each stage, enough correction masses to ensure that the lower modes do not again become unbalanced.

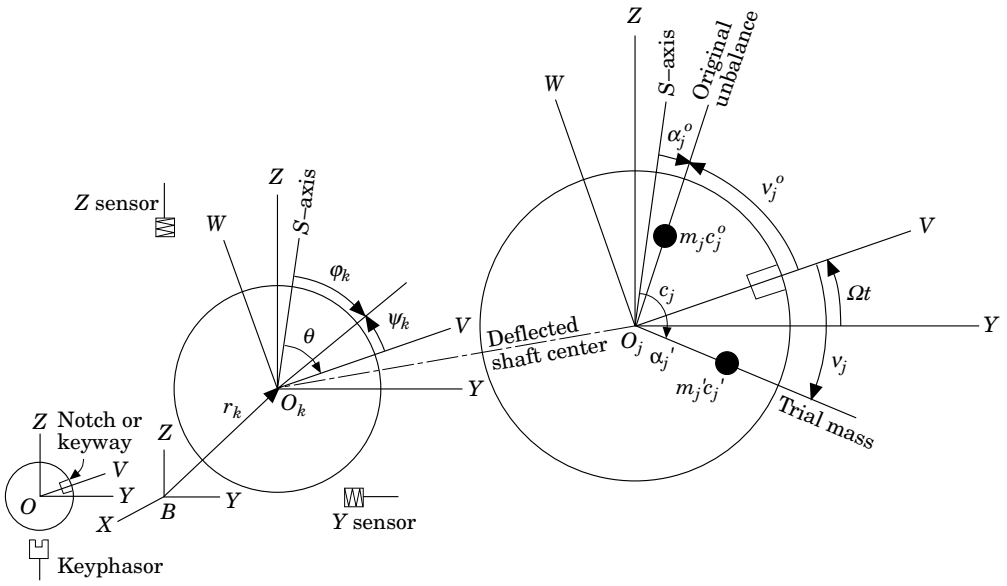

Figure 2. A scheme of a typical element. (a) The kth measurement point; (b) the jth balancing plane.

In balancing operations the whirl response, the rotating force of the trial mass and the rotating force of the unbalance can all be described by vectors which are rotating at a constant spin speed. With an angular position as a reference (such as a keyway or notch), rotating vectors and influence coefficients with respect to the rotating frame of reference can be expressed by complex variables. Two typical points, one located at a measurement position and another located at a balancing plane, are shown in Figure 2. The geometric center O_k of the element at the kth measurement point is displaced from the bearing center B by r_k. The rotating reference is denoted by the V-axis. The unknown angular position of unbalance of an appointed plane is denoted by the S-axis. In the rotating reference frame phases of the original unbalance distribution, trial masses, and measured responses may be defined relative to the S-axis as α_j^0, α_j' and φ_k respectively. Beforehand, these angles and the S-axis are unknown. However, the angle θ measured from the V-axis to the S-axis can be determined as described below. In addition, one may define phases of these rotating vectors relative to the V-axis by v_j and ψ_k respectively. These angles can be obtained by measurements. Any one balancing plane may be used to locate the S-axis. For example, if $j = 1$, then $\alpha_1 = 0$ and $\theta = v_1$; and other relative phases of unbalance, such as that of the jth plane α_j, are determined by

$$\alpha_j = \theta - v_j, \tag{19a}$$

where v_j is obtained by a measurement of the angle relative to the V-axis. Also, the angles of the unbalance response can be related by

$$\varphi_k = \theta - \psi_k, \tag{19b}$$

where θ and φ_k are angles relative to the S-axis, and ψ_k is the angle relative to the V-axis. The phase ψ_k can be measured with respect to the rotating reference.

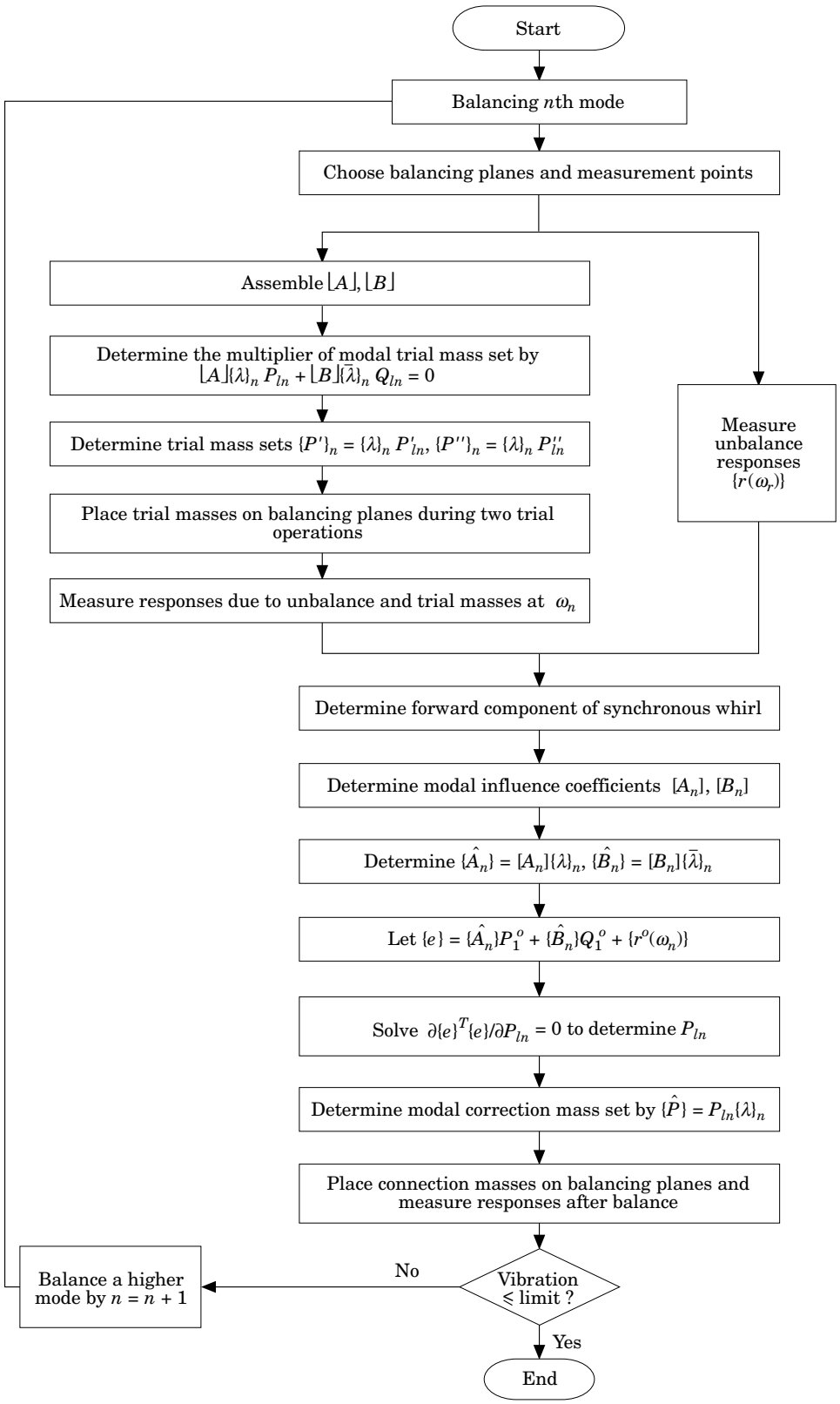

Figure 3. The flowchart of the unified balancing process.

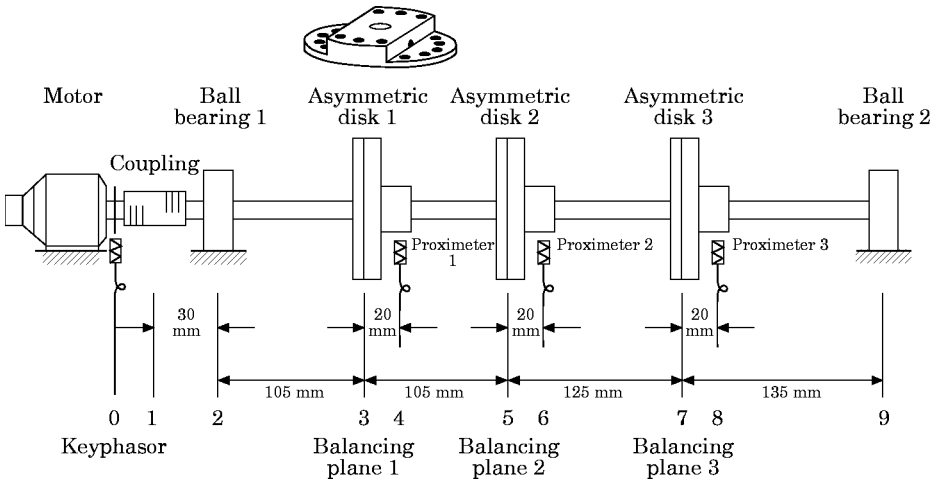

Figure 4. An experimental apparatus.

In the rotating frame the unbalance force at the jth plane can be expressed by

$$P_j = \Omega^2 m_j c_j e^{-i\alpha_j} = (P_{vj} + iP_{wj})\, e^{-i\theta} \tag{20a}$$

at the balancing speed Ω, where $P_{vj} + iP_{wj} = \Omega^2 m_j c_j e^{-iv}$. The measured response of the kth point due to the unbalance force is

$$r_k = R_k e^{-i\varphi_k} = R_k e^{-i(\theta - \psi_k)} = (g_k + i\gamma_k)\, e^{-i\theta} \tag{20b}$$

where $g_k + i\gamma_k = R_k\, e^{i\psi_k}$.

Substituting equations (20a) and (20b) into (6) gives

$$r_k = g_k + i\gamma_k = \sum_{j=1}^{J} (A_{kj}P_j + B_{kj}Q_j). \tag{21}$$

The relationship between the whirl response and the original unbalance thus can be derived from equation (21), i.e.,

$$\sum_{j=1}^{J} (A_{kj}P_j^o + B_{kj}Q_j^o) = g_k^o + i\gamma_k^o. \tag{22}$$

By considering the addition of the trial masses at J balancing planes, one can obtain

$$\sum_{j=1}^{J} [A_{kj}(P_j^o + P_j') + B_{kj}(Q_j^o + Q_j')] = g_k' + i\gamma_k' \tag{23}$$

due to the trial masses $m_j' c_j'$, $j = 1, 2, \ldots, J$, and

$$\sum_{j=1}^{J} [A_{kj}(P_j^o + P_j'') + B_{kj}(Q_j^o + Q_j'')] = g_k'' + i\gamma_k'' \tag{24}$$

due to another trial mass set $m_j'' c_j'', j = 1, 2, , \ldots, J$. Subtracting equation (23) from equation (22), and equation (24) from equation (22), one obtains the following equations:

$$(A_{kj}^{\mathrm{R}} + B_{kj}^{\mathrm{R}})(P_v')_j + (-A_{kj}^{\mathrm{I}} + B_{kj}^{\mathrm{I}})(P_w')_j = g_k' - g_k^o,$$

$$(A_{kj}^{\mathrm{I}} + B_{kj}^{\mathrm{I}})(P_v')_j + (A_{kj}^{\mathrm{R}} - B_{kj}^{\mathrm{R}})(P_w')_j = \gamma_k' - \gamma_k^o,$$

$$(A_{kj}^{\mathrm{R}} + B_{kj}^{\mathrm{R}})(P_v'')_j + (-A_{kj}^{\mathrm{I}} + B_{kj}^{\mathrm{I}})(P_w'')_j = g_k'' - g_k^o,$$

$$(A_{kj}^{\mathrm{I}} + B_{kj}^{\mathrm{I}})(P_v'')_j + (A_{kj}^{\mathrm{R}} - B_{kj}^{\mathrm{R}})(P_w'')_j = \gamma_k'' - \gamma_k^o. \tag{25}$$

These non-homogeneous equations (25) can be solved to determine the modal influence coefficients which relate the unbalance forces of J balancing planes to the responses of K measured points at the nth critical speed.

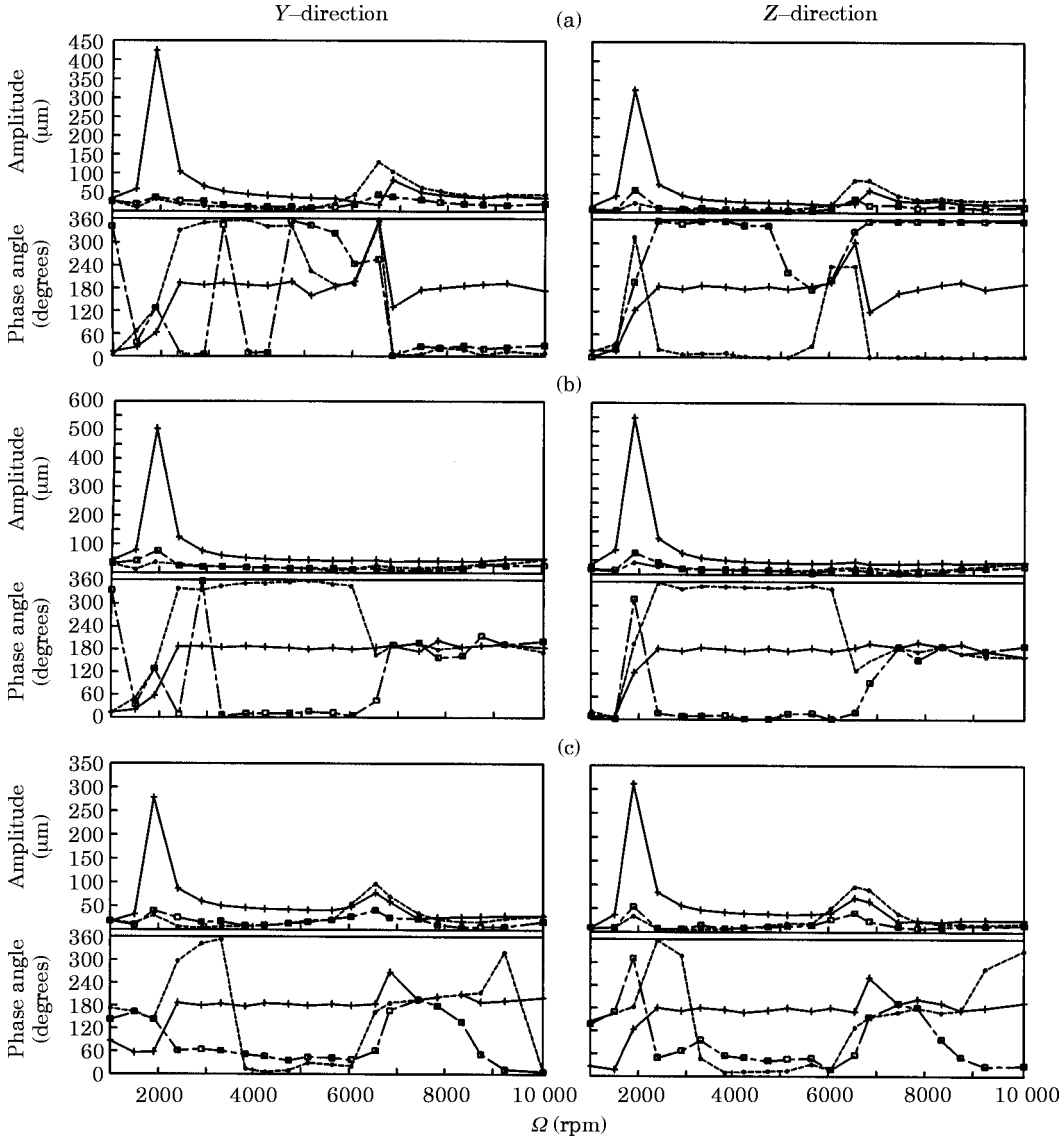

Figure 5. The whirl responses of the experiment. Measurement at (a) point 4, (b) point 6 and (c) point 8. — + —, before balancing; ——●——, after balancing the first mode; –·–□–·–, after balancing the second mode.

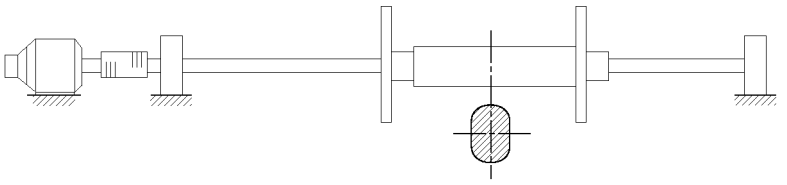

(a)

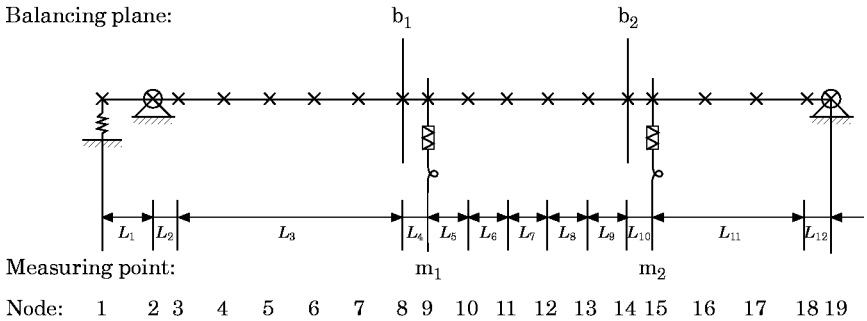

(b)

Figure 6. The rotor–bearing system of the numerical examples. (a) The rotor kit; (b) the finite element model.

When a bearing is non-axisymmetrical, the measuring or balancing positions are chosen points not located on the bearing. The first trial mass is related to the forward component by influence coefficients as follows:

$$A_{kj}P'_j + B_{kj}Q'_j = f'_k - f^o_k. \tag{26a}$$

Similarly, the second trial operation gives

$$A_{kj}P''_j + B_{kj}Q''_j = f''_k - f^o_k, \tag{26b}$$

where f^o, f' and f'' are the forward components due to the original unbalance, the first trial operation and the second trial operation respectively. Equations (26a) and (26b) were verified and demonstrated in detail by Kang *et al*. [19].

One may define $\{\hat{A}_n\}$ and $\{\hat{B}_n\}$ to be obtained by post-multiplying $[A_n]$ and $[B_n]$ by $\{\lambda\}_n$ and $\{\bar{\lambda}\}_n$ respectively. Equation (22) can be alternatively expressed by

$$\{\hat{A}_n\}P^o_{1n} + \{\hat{B}_n\}Q^o_{1n} = \{r^o_n\} \tag{27a}$$

for systems having isotropic bearings, and

$$\{\hat{A}_n\}P^o_{1n} + \{\hat{B}_n\}Q^o_{1n} = \{f^o_n\} \tag{27b}$$

for systems having non-axisymmetrical bearings, where P^o_{1n} and Q^o_{1n} are original unbalance components of the nth mode and themselves complex conjugates in the reference plane, $\{r^o_n\}$ is the measurement of the synchronous whirl at the nth mode, and $\{f^o_n\}$ is a vector of forward components.

If measurements of whirl response are made at only one location, the modal influence coefficient vectors $\{\hat{A}_n\}$ and $\{\hat{B}_n\}$ include one element. It appears that the correction masses

of P^o_{1n} and Q^o_{1n} can be obtained by one calculation. In practice, unbalance response is measured at more planes than this, and a process is used to determine the optimum correction. This optimization is to minimize the error of

$$\{e\} = \{\hat{A}_n\}P^o_{1n} + \{\hat{B}_n\}Q^o_{1n} - \{r^o_n\} \tag{28a}$$

or

$$\{e\} = \{\hat{A}_n\}P^o_{1n} + \{\hat{B}_n\}Q^o_{1n} - \{f^o_n\}. \tag{28b}$$

The flowchart for this modified unified method is shown in Figure 3. This figure is constructed by the modification of those obtained by Parkinson *et al*. [15], Darlow *et al*. [16] and Darlow [17, 18]. Consequently, with an unsymmetrical rotor–bearing system which has several critical speeds, within its operating speed range, this modified unified method is applied in a graduated process in which each mode of unbalance is corrected in turn by means of whirl measurements made at balancing speeds approximating the corresponding critical speeds, so that simultaneous calculations can be made through equations (15b), (25) and (28). Once the P^o_{1n} of the nth mode is determined, the correction mass set is thus obtained by

$$\{P\}_n = \{\lambda\}_n P^o_{1n}. \tag{29}$$

TABLE 1

Details of the numerical examples

Symmetric shaft:
$\Psi_v = \Psi_w = 4{\cdot}049 \times 10^{-10}\ \mathrm{m}^4$, $d = 9{\cdot}53\ \mathrm{mm}$, $\rho = 7850\ \mathrm{kg/m}^3$, $E = 2 \times 10^{11}\ \mathrm{N/m}^2$,
$A = 7{\cdot}133 \times 10^{-5}\ \mathrm{m}^2$, $L_2 = L_4 = L_{10} = L_{12} = 0{\cdot}015\ \mathrm{m}$,
$L_1 = 0{\cdot}03\ \mathrm{m}$, $L_3 = 0{\cdot}135\ \mathrm{m}$, $L_{11} = 0{\cdot}092\ \mathrm{m}$

Asymmetric shaft:
$\Psi_v = 6{\cdot}642 \times 10^{-10}\ \mathrm{m}^4$, $\Psi_w = 2{\cdot}546 \times 10^{-10}\ \mathrm{m}^4$, $\rho = 7850\ \mathrm{kg/m}^3$, $E = 2 \times 10^{11}\ \mathrm{N/m}^2$,
$A = 2{\cdot}2470 \times 10^{-4}\ \mathrm{m}^2$, $L_5 = L_6 = L_7 = L_8 = L_9 = 0{\cdot}024\ \mathrm{m}$

Disk at node 4, 10:
$I^d_v = I^d_w = 1{\cdot}61 \times 10^{-4}\ \mathrm{kg\,m}^2$, $J^d = 3{\cdot}02 \times 10^{-4}\ \mathrm{kg\,m}^2$, $m^d = 0{\cdot}4127\ \mathrm{kg}$

Cylinders at node 5, 11:
$I^d_v = 7{\cdot}91 \times 10^{-6}\ \mathrm{kg\,m}^2$, $I^d_w = 7{\cdot}79 \times 10^{-6}\ \mathrm{kg\,m}^2$, $m^d = 0{\cdot}0806\ \mathrm{kg}$, $J^d = 7{\cdot}32 \times 10^{-6}\ \mathrm{kg\,m}^2$

Bearing at node 2, 13:
$K_{yy} = K_{zz} = 10^7\ \mathrm{N/m}$, $K_{yz} = K_{zy} = 0$, $C_{yy} = C_{zz} = 1000\ \mathrm{N\,s/m}$, $C_{yz} = C_{zy} = 0$,

Spring coupling at node 1:
$K_{yy} = K_{zz} = 10^3\ \mathrm{N/m}$, $K_{yz} = K_{zy} = C_{yy} = C_{zz} = C_{yz} = C_{zy} = 0$

Unbalance distribution (g mm) at nodes $\mu_j = m_j c_j$:
$\mu_3 = 1{\cdot}6 \angle -16^\circ$, $\mu_4 = 1{\cdot}4 \angle -14^\circ$, $\mu_5 = 1{\cdot}3 \angle -13^\circ$, $\mu_6 = 1{\cdot}8 \angle -18^\circ$,
$\mu_7 = 2{\cdot}0 \angle -20^\circ$, $\mu_8 = 22 \angle -61{\cdot}5^\circ$, $\mu_9 = 4{\cdot}6 \angle -46^\circ$, $\mu_{10} = 3{\cdot}6 \angle -36^\circ$,
$\mu_{11} = 3{\cdot}4 \angle -34^\circ$, $\mu_{12} = 3{\cdot}5 \angle -35^\circ$, $\mu_{13} = 2{\cdot}3 \angle -23^\circ$, $\mu_{14} = 24 \angle -18{\cdot}6^\circ$,
$\mu_{15} = 3{\cdot}8 \angle -38^\circ$, $\mu_{16} = 1{\cdot}8 \angle -18^\circ$, $\mu_{17} = 1{\cdot}5 \angle -15^\circ$, $\mu_{18} = 1{\cdot}2 \angle -12^\circ$,

Residual permanent deflections at nodes (μm):
$\mathrm{r}_1 = -41 \angle 0^\circ$, $\mathrm{r}_3 = 15 \angle 0^\circ$, $\mathrm{r}_4 = 48 \angle 0^\circ$, $\mathrm{r}_5 = 62 \angle 0^\circ$, $\mathrm{r}_6 = 78 \angle 0^\circ$,
$\mathrm{r}_7 = 90 \angle 0^\circ$, $\mathrm{r}_8 = 94 \angle 0^\circ$, $\mathrm{r}_9 = 98 \angle 0^\circ$, $\mathrm{r}_{10} = 100 \angle 0^\circ$, $\mathrm{r}_{11} = 99 \angle 0^\circ$,
$\mathrm{r}_{12} = 97 \angle 0^\circ$, $\mathrm{r}_{13} = 94 \angle 0^\circ$, $\mathrm{r}_{14} = 90 \angle 0^\circ$, $\mathrm{r}_{15} = 80 \angle 0^\circ$, $\mathrm{r}_{16} = 65 \angle 0^\circ$,
$\mathrm{r}_{17} = 38 \angle 0^\circ$, $\mathrm{r}_{18} = 18 \angle 0^\circ$, $\mathrm{r}_{19} = 0 \angle 0^\circ$,

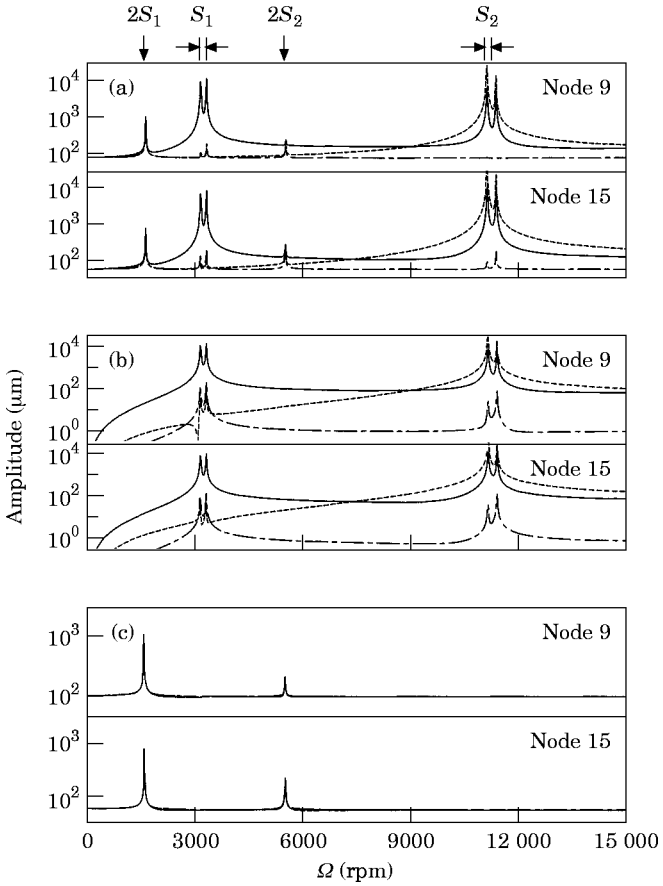

Figure 7. The steady state responses of the numerical model without residual permanent deflection. (a) Peak-to-peak amplitudes; (b) synchronous responses; (c) double-frequency responses. ——, Before balancing; ----, after balancing the first mode; – – –, after balancing the second mode.

5. EXPERIMENTAL AND NUMERICAL EXAMPLES

The experimental apparatus is shown in Figure 4. An axisymmetrical shaft 490 mm in length and 9·53 mm in diameter, made of medium-carbon steel, was supported by two ball bearings at both ends. Two non-axisymmetrical disks and two axisymmetrical cylinders were mounted on the shaft as shown. The disks had a mass of $m^d = 0{\cdot}5464$ kg, a polar moment of inertia of $J^d = 3{\cdot}37 \times 10^{-4}$ kg m^2 and diametrical moments of inertia of $I_v^d = 2{\cdot}58 \times 10^{-4}$ kg m^2 and $I_w^d = 1{\cdot}42 \times 10^{-4}$ kg m^2 about the two principal axes of the disk. The cylinders had corresponding measurements of $m^d = 0{\cdot}0806$ kg, $J^d = 7{\cdot}32 \times 10^{-6}$ kg m^2 and $I_v^d = I_w^d = 7{\cdot}85 \times 10^{-6}$ kg m^2.

The rotating reference was a notch on a thin disk mounted at point 0 and recorded by a keyphasor at each rotation, and deflections at points 4, 6 and 8 were measured by proximity probes in mutually perpendicular directions. Since this shaft was made by cutting both sides of a steel bar having a circular cross-section, an initial bend in the shape was likely to occur. This assembly was experimentally balanced by correction masses on three balancing planes at points 3, 5 and 7.

Two modifications were made: (a) two trial masses were applied at two different positions for the same balancing plane; and (b) the forward components were utilized to determine the influence coefficients and the unbalance distribution. The experimental

results of balancing this apparatus using only one modification are shown by Kang *et al*. [19]. They show that the approaches with either the (a) or the (b) modification cannot provide an equivalent unbalance distribution for correction. Thus, neutralization/cancellation of the vibrations cannot be attained through these improper corrections. Furthermore, the vibrations become more severe when approaching speeds in the vicinity of the second mode.

With the use of both modifications, the modal influence coefficients and the correction masses of the first and the second modes are determined. According to the computational results, the correction mass was applied to the second disk for balancing the first mode, and the correction masses were applied to the first and the third disks, respectively, for balancing the second mode, respectively. The plots of the peak-to-peak response due to the experimental results are shown in Figure 5. After balancing the first mode, the unbalance responses cannot be reduced within the speed regions in the vicinity of the second mode. However, after the completion of the second mode balancing, the vibration at all speed ranges was reduced to a reasonable level. During measurement, the secondary resonant peaks are not present at point 6. The reason is that the point is located at a node of the second mode.

The numerical example is as shown in Figure 6. A partially non-axisymmetrical shaft is supported by rolling bearings at both ends. Two axisymmetrical disks and two cylinders are mounted on the shaft as shown. It is assumed that the unbalance is distributed discretely at each node. The physical parameters of this system are listed in Table 1. There are two balancing planes at points b_1 and b_2 and two measuring points at points m_1 and m_2. In the first case this system is considered without residual permanent deflection.

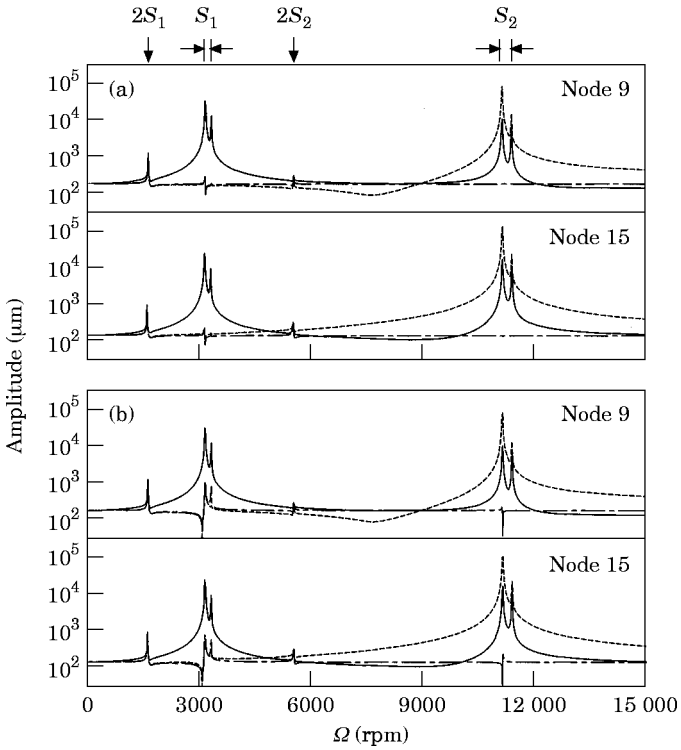

Figure 8. The peak-to-peak responses of the numerical model with residual permanent deflection. (a) Balance of the response caused by unbalance; (b) balance of the total shaft deflection to zero. Key as Figure 7.

For balancing the first mode plane b_1, the critical speed 3132 rpm of the first mode is utilized. One may determine modal influence coefficients by two trial operations without determining the trial mass multiplier set. The modal influence coefficients listed in Appendix B relate the measured response at point m_1 and one mass at point b_1. By substituting the simulated unbalance response of point m_1 into equation (27), $P_1 = 6{\cdot}37 \times 10^{-5}$ kg m, $\angle -99^\circ$ of the correction mass are obtained.

For balancing the second mode, modal influence coefficients of the first mode are used to determine the modal trial mass multiplier set. This set is obtained from equation (15b) and shown as $\lambda_1 = 1$, and $\lambda_2 = 1{\cdot}259$, $\angle -179{\cdot}73^\circ$.

Using the modal trial mass set, the modal influence coefficients of the second mode are determined by equation (27a) and also listed in Appendix A. By substituting the simulated unbalance responses of points m_1 and m_2 into equation (27a), $P_1 = 2{\cdot}9670 \times 10^{-5}$ kg m, $\angle -23{\cdot}14^\circ$ and $P_2 = 3{\cdot}6836 \times 10^{-5}$ kg m, $\angle 156{\cdot}98^\circ$ of the correction masses at planes b_1 and b_2 are obtained.

This system is balanced by the modified unified method, and in Figure 7 are shown steady state responses within the range of angular velocity 0–15 000 rpm of nodes 9 and 15. In this figure solid lines show the whirl responses before balancing, dashed lines show the responses after balancing the first mode and chain lines show the responses after balancing the second mode. At the top of this figure, S_n and $2S_n$ denotes the synchronous resonance and the $2\times$ subcritical resonance of the nth mode for resonant peaks.

In Figure 7(a) are shown the peak-to-peak amplitudes of the vibrations, which contain synchronous and double-frequency whirls as shown in Figures 7(b) and 7(c), respectively. The synchronous whirl due to the residual unbalance or residual permanent deflection has

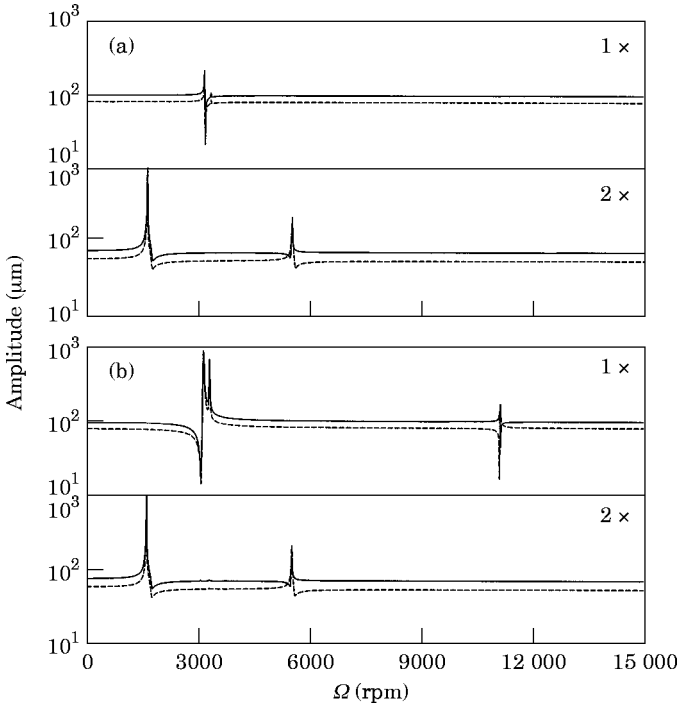

Figure 9. The synchronous and double-frequency responses after balancing the second mode in the case of Figure 8. (a) To balance the response caused by unbalance; (b) to balance the total shaft deflection to zero. $1\times$, Synchronous whirl; $2\times$, double-frequency whirl. —, Node 9; ----, node 15.

a frequency equal to the angular speed and its amplitude depends on the residual unbalance and the residual permanent deflection. Resonances due to this excitation appear for an angular speed equal to one of the natural frequencies of the rotor $\omega_n = \Omega$. This response can be attenuated by means of the correction masses attached in the balancing planes. The superharmonic whirl due to gravity forces (which exist only for horizontal rotors) has a frequency equal to twice the angular speed and its amplitude depends on the coefficient of the parametric excitation (not on the residual unbalance). Resonances due to this excitation appear for an angular speed equal to half of the natural frequency of the rotor $\omega_n = 2\Omega$. This response cannot be attenuated by means of the correction masses.

As shown in Figure 7(b), the amplitude of the synchronous whirl after balancing the second mode is almost cancelled within range of angular velocity of 0–15 000 rpm, excluding the vicinities of two main modes. As shown in Figure 7(c), two resonant peaks at half the first and second critical speeds are caused by the corresponding subcritical resonances. These peaks are decreased by removing the correction mass, and increased by adding the correction masses. However, it is not possible completely to eliminate these peaks by a balancing operation.

The same model, however, with the residual permanent deflection, also shown in Table 1, is considered. Two balancing approaches based on the work of Nicholas *et al*. [22] are utilized for this case: both approaches use the critical speeds as balancing speeds. These are (a) only balancing the unbalance response to zero and (b) balancing the total shaft deflection to zero, and the balancing results presented as peak-to-peak amplitudes are shown in Figures 8(a) and 8(b), respectively. The amplitudes of synchronous and double-frequency responses after balancing the second mode are shown in Figure 9. The residual responses of both approaches are mainly induced by the residual permanent deflection and the double speed whirl. Consequently, the responses due to residual unbalance are attenuated approximately to zero at speeds other than the critical speeds.

6. CONCLUSIONS

This study has shown how the modal influence coefficient matrices of unsymmetrical rotor–bearing systems can be derived by the finite element formulation. During the formulation it was also found that two trial operations and forward precessions calculated from the measurement of unbalanced responses are requisite steps for the determination of the unbalance.

On the basis of a theoretical introduction, a modified unified method was developed for balancing unsymmetrical rotor–bearing systems. By the use of this method, the modes can be balanced individually, without affecting the balance in lower modes which have already been balanced. The experimental and simulated results of the numerical examples demonstrate the superiority of this modification of the unified balancing approach.

ACKNOWLEDGMENT

This study was supported by the National Science Council of the Republic of China, under grant number NSC 82-0424-E-033-060.

REFERENCES

1. E. L. Thearle 1934 *Transactions of the American Society of Mechanical Engineers*, *Journal of Applied Mechanics* **56**, 745–753. Dynamic balancing of rotating machinery in the field.
2. J. G. Baker 1939 *Transactions of the American Society of Mechanical Engineers*, *Journal of Applied Mechanics* **61**, A1–A6. Methods of rotor-unbalance determination.

3. T. P. Goodman 1964 *Transactions of the American Society of Mechanical Engineers*, *Journal of Engineering for Industry* **86**, 273–279. A least-squares method for computing balance corrections.
4. J. W. Lund and J. Tonneson 1972 *Transactions of the American Society of Mechanical Engineers*, *Journal of Engineering for Industry* **94**(1), 233–242. Analysis and experiments on multi-plane balancing of a flexible rotor.
5. J. M. Tessarzik, R. H. Badgley and W. J. Anderson 1972 *Transactions of the American Society of Mechanical Engineers*, *Journal of Engineering for Industry*, 148–158. Flexible rotor balancing by the exact point-speed influence coefficient method.
6. J. M. Tessarzik, R. H. Badgley and D. P. Fleming 1976 *Transactions of the American Society of Mechanical Engineers*, *Journal of Engineering for Industry*, 988–998. Experimental evaluation of multiplane-multispeed rotor balancing through multiple critical speeds.
7. W. D. Pilkey and J. T. Bailey 1979 *Transactions of the American Society of Mechanical Engineers*, *Journal of Mechanical Design* **101**(2), 304–308. Constrained balancing techniques for flexible rotors.
8. W. D. Pilkey, J. T. Bailey and P. D. Smith 1983 *Transactions of the American Society of Mechanical Engineers*, *Journal of Vibration*, *Acoustics*, *Stress*, *and Reliability in Design* **105**, 90–93. A computational technique for optimizing correction weights and axial location of balance planes of rotating shafts.
9. R. E. D. Bishop and G. M. L. Gladwell 1959 *Journal of Mechanical Engineering Science* **1**, 66–77. The vibration and balancing of an unbalanced flexible rotor.
10. R. E. D. Bishop and A. G. Parkinson 1972 *Transactions of the American Society of Mechanical Engineers*, *Journal of Engineering for Industry*, 561–576. Balancing machines for flexible rotors.
11. A. G. Parkinson, K. L. Jackson and R. E. D. Bishop 1963 *Journal of Mechanical Engineering Science* **5**, 114–128. Some experiments on the balancing of small flexible rotors: part I—theory.
12. A. G. Parkinson, K. L. Jackson and R. E. D. Bishop 1963 *Journal of Mechanical Engineering Science* **5**, 133–145. Some experiments on the balancing of small flexible rotors: part II—experiments.
13. S. Saito and T. Azuma 1983 *Transactions of the American Society of Mechanical Engineers*, *Journal of Vibration*, *Acoustics*, *Stress and Reliability in Design* **15**, 94–100. Balancing of flexible rotors by the complex modal method.
14. W. L. Meacham, P. B. Talbert, H. D. Nelson and N. K. Cooperrider 1988 *American Institute of Aeronautics and Astronautics*, *Journal of Propulsion and Power* **4**(3), 245–251. Complex modal balancing of flexible rotors including residual bow.
15. A. G. Parkinson, M. S. Darlow and A. J. Smalley 1980 *Journal of Sound and Vibration* **68**, 489–506. A theoretical introduction to the development of a unified approach to flexible rotor balancing.
16. M. S. Darlow, A. J. Smalley and A. G. Parkinson 1981 *Transactions of the American Society of Mechanical Engineers*, *Journal of Engineering for Power* **103**, 101–107. Demonstration of a unified approach to the balancing of flexible rotors.
17. M. S. Darlow 1987 *Mechanical Systems and Signal Processing* **1**(1), 105–134. Balancing of high-speed machinery: theory, methods and experimental results.
18. M. S. Darlow 1989 *Balancing of High-speed Machinery*. New York: Springer-Verlag.
19. Y. Kang, C. P. Liu and G. J. Sheen 1996 *Journal of Sound and Vibration* **194**, 199–218. A modified influence coefficient method for balancing unsymmetrical rotor–bearing systems.
20. H. D. Nelson 1985 *Transactions of the American Society of Mechanical Engineers*, *Journal of Vibration*, *Acoustics*, *Stress*, *and Reliability in Design* **107**, 460–461. Rotor dynamics equations in complex form.
21. G. Genta 1988 *Journal of Sound and Vibration* **124**, 27–53. Whirling of unsymmetrical rotors: a finite-element approach based on complex coordinates.
22. J. C. Nicholas, E. J. Gunter and P. E. Allaire 1976 *Transactions of the American Society of Mechanical Engineers*, *Journal of Engineering for Power* **98**, 182–189. Effect of residual shaft bow on unbalance response and balancing of a single flexible rotor, part II: balancing.

APPENDIX A

The modal influence coefficients are listed as follows:

$$A_{9,8} = 11{\cdot}4131\ \mathrm{kg}^{-1} \angle 0{\cdot}1334^{\circ}$$

$$\hat{B}_{9,8} = 5{\cdot}7714\ \mathrm{kg}^{-1} \angle -0{\cdot}0106^{\circ}$$

for the first mode, and

$$\hat{A}_{9,8} = 11{\cdot}4130\ \mathrm{kg}^{-1} \angle 0{\cdot}1334^\circ, \qquad \hat{A}_{9,14} = 9{\cdot}1267\ \mathrm{kg}^{-1} \angle 0{\cdot}1374^\circ,$$

$$\hat{A}_{15,8} = 8{\cdot}5463\ \mathrm{kg}^{-1} \angle 0{\cdot}1393^\circ, \qquad \hat{A}_{15,14} = 7{\cdot}0568\ \mathrm{kg}^{-1} \angle 0{\cdot}1395^\circ,$$

$$\hat{B}_{9,8} = 5{\cdot}5771\ \mathrm{kg}^{-1} \angle -0{\cdot}0011^\circ, \qquad \hat{B}_{9,14} = 4{\cdot}5801\ \mathrm{kg}^{-1} \angle -0{\cdot}0016^\circ,$$

$$\hat{B}_{15,8} = 4{\cdot}2489\ \mathrm{kg}^{-1} \angle 0{\cdot}0236^\circ, \qquad \hat{B}_{15,14} = 3{\cdot}4930\ \mathrm{kg}^{-1} \angle 0{\cdot}0018^\circ,$$

for the second mode.

APPENDIX B: NOTATION

A_{kj}, B_{kj}	element in the kth row and the jth column of matrices $[A]$ and $[B]$
$[A]$, $[B]$	influence coefficient matrices
c, m	eccentricity, mass
$\{e\}$	error function
f, b	relative components of forward precession and a backward precession to a rotating reference, respectively
$\{F\}$	nodal force vector relative to (UVW)
g, γ	real, imaginary part of r
i	$\sqrt{-1}$
J, K	number of balancing planes, measuring points
$[K]$, $[C]$	stiffness, damping matrix
$[M]$, $[G]$	mass, gyroscopic matrix
$\{p\}$	displacement vector relative to (UVW)
$\{P\}$, $\{Q\}$	complex form and conjugate of $\{F\}$
q	synchronous whirl
r	translations in a complex form
R	amplitude of r
S_n, $2S_n$	synchronous and $2\times$ resonance of the nth mode
$\{r\}$	complex form of $\{p\}$
(UVW)	the rotating reference frame fixed on the principal axes of the shaft, with U as the spin axis
v, w	translations in V and W directions
(XYZ)	the inertial frame of reference with X being fixed on U
y, z	translations in Y and Z directions
α, ν	the angular position of an unbalance relative to the specific original unbalance, relative to the rotating referenced location, respectively
θ_v, θ_w	rotations about the V- and W-axes
φ	phase lag of response relative to unbalance
θ	the relative angle of appointed unbalanced measured from a rotating reference
Ω	rotating speed or balancing speed
ω_n	critical speed of the nth mode
λ, $\{\lambda\}$	complex multiplier of trial masses or correction masses, the vector of the multiplier set
ψ	the phase of the response measured from a rotating reference

Superscripts

o	original unbalance
R, I	real part and imaginary part of a complex variable
$'$	trial mass, the first time
$''$	trial mass, the second time
$\bar{}$	complex conjugate

Subscripts

c, s	cosine term, sine term
j, k	the jth measurement point, the kth balancing plane
r	rotating
v, w	components in the V and W directions
n	the order of resonant modes